Throughput Maximization in Wireless Powered Communication Networks

Hyungsik Ju and Rui Zhang

arXiv:1304.7886v4 [cs.IT] 21 Jul 2014

Abstract

This paper studies the newly emerging wireless powered communication network in which one hybrid access point (H-AP) with constant power supply coordinates the wireless energy/information transmissions to/from a set of distributed users that do not have other energy sources. A "harvest-then-transmit" protocol is proposed where all users first harvest the wireless energy broadcast by the H-AP in the downlink (DL) and then send their independent information to the H-AP in the uplink (UL) by time-division-multiple-access (TDMA). First, we study the sum-throughput maximization of all users by jointly optimizing the time allocation for the DL wireless power transfer versus the users' UL information transmissions given a total time constraint based on the users' DL and UL channels as well as their average harvested energy values. By applying convex optimization techniques, we obtain the closed-form expressions for the optimal time allocations to maximize the sum-throughput. Our solution reveals an interesting "doubly near-far" phenomenon due to both the DL and UL distance-dependent signal attenuation, where a far user from the H-AP, which receives less wireless energy than a nearer user in the DL, has to transmit with more power in the UL for reliable information transmission. As a result, the maximum sum-throughput is shown to be achieved by allocating substantially more time to the near users than the far users, thus resulting in unfair rate allocation among different users. To overcome this problem, we furthermore propose a new performance metric so-called common-throughput with the additional constraint that all users should be allocated with an equal rate regardless of their distances to the H-AP. We present an efficient algorithm to solve the common-throughput maximization problem. Simulation results demonstrate the effectiveness of the common-throughput approach for solving the new doubly near-far problem in wireless powered communication networks.

Index Terms

Wireless power, energy harvesting, throughput maximization, doubly near-far problem, TDMA, convex optimization.

I. Introduction

Traditionally, energy-constrained wireless networks, such as sensor networks, are powered by fixed energy sources, e.g. batteries, which have limited operation time. Although the lifetime of the network can be extended by replacing or recharging the batteries, it may be inconvenient, costly, dangerous (e.g.,

H. Ju is with the Department of Electrical and Computer Engineering, National University of Singapore (e-mail: elejhs@nus.edu.sg).

R. Zhang is with the Department of Electrical and Computer Engineering, National University of Singapore (e-mail: elezhang@nus.edu.sg). He is also with the Institute for Infocomm Research, A*STAR, Singapore.

in a toxic environment) or even impossible (e.g., for sensors implanted in human bodies). As an alternative solution to prolong the network's lifetime, energy harvesting has recently drawn significant interests since it potentially provides unlimited power supplies to wireless networks by scavenging energy from the environment.

In particular, radio signals radiated by ambient transmitters become a viable new source for wireless energy harvesting. It has been reported that 3.5mW and 1uW of wireless power can be harvested from radio-frequency (RF) signals at distances of 0.6 and 11 meters, respectively, using Powercast RF energy-harvester operating at 915MHz [1]. Furthermore, recent advance in designing highly efficient rectifying antennas will enable more efficient wireless energy harvesting from RF signals in the near future [2]. It is worth noting that there has been recently a growing interest in studying wireless powered communication networks (WPCNs), where energy harvested from ambient RF signals is used to power wireless terminals in the network, e.g., [3]-[5]. In [3], a wireless powered sensor network was investigated, where a mobile charging vehicle moving in the network is employed as the energy transmitter to wirelessly power the sensor nodes. In [4], the wireless powered cellular network was studied in which dedicated power-beacons are deployed in the cellular network to charge mobile terminals. Moreover, the wireless powered cognitive radio network has been considered in [5], where active primary users are utilized as energy transmitters for charging their nearby secondary users that are not allowed to transmit over the same channel due to strong interference. Furthermore, since radio signals carry energy as well as information at the same time, a joint investigation of simultaneous wireless information and power transfer (SWIPT) has recently drawn a significant attention (see e.g. [6]-[11] and the references therein).

In this paper, we study a new type of WPCN as shown in Fig. 1, in which one hybrid access point (H-AP) with constant power supply (e.g. battery) coordinates the wireless energy/information transmissions to/from a set of distributed users that are assumed to have no other energy sources. All users are each equipped with a rechargeable battery and thus can harvest and store the wireless energy broadcast by the H-AP. Unlike prior works on SWIPT [6]-[11], which focused on the simultaneous energy and information transmissions to users in the downlink (DL), in this paper we consider a different setup where the H-AP broadcasts only wireless energy to all users in the DL while the users transmit their independent information using their individually harvested energy to the H-AP in the uplink (UL). We are interested in maximizing the UL throughput of the aforementioned WPCN by optimally allocating the time for the

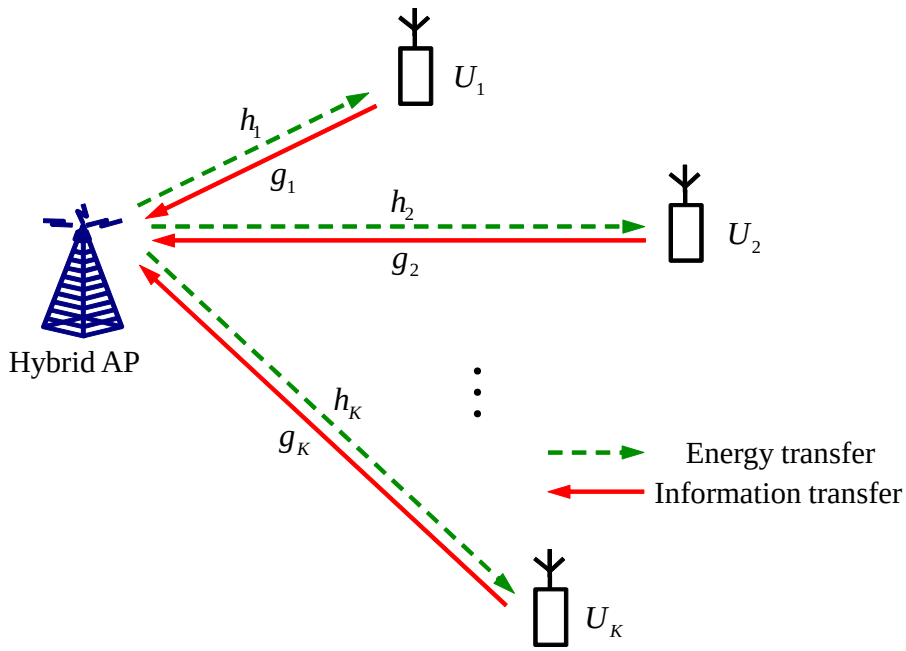

Fig. 1. A wireless powered communication network (WPCN) with wireless energy transfer (WET) in the downlink (DL) and wireless information transmissions (WITs) in the uplink (UL).

DL wireless energy transfer (WET) by the H-AP and the UL wireless information transmissions (WITs) by different users.

The main contributions of this paper are summarized as follows:

- We propose a protocol termed "harvest-then-transmit" for the WPCN depicted in Fig. 1, where the H-AP first broadcasts wireless energy to all users in the DL, and then the users transmit their independent information to the H-AP in the UL using their individually harvested energy by time-division-multiple-access (TDMA).
- With the proposed protocol, we first maximize the sum-throughput of the WPCN by jointly optimizing the time allocated to the DL WET and the UL WITs given a total time constraint, based on the users' DL and UL channels as well as their average harvested energy amount. It is shown that the sum-throughput maximization problem is convex, and therefore we derive closed-form expressions for the optimal time allocations by applying convex optimization techniques [12].
- Our solution reveals an interesting new "doubly near-far" phenomenon in the WPCN, when a far user from the H-AP receives less amount of wireless energy than a nearer user in the DL, but has to transmit with more power in the UL for achieving the same information rate due to the doubly distance-dependent signal attenuation in both the DL WET and UL WIT. Consequently, the sum-

throughput maximization solution is shown to allocate substantially more time to the near users than the far users, thus resulting in unfair achievable rates among different users.

- To overcome the doubly near-far problem, we furthermore propose a new performance metric referred to as *common-throughput* with the additional constraint that all users should be allocated with an equal rate in their UL WITs regardless of their distances to the H-AP. We propose an efficient algorithm to maximize the common-throughput of the WPCN by re-optimizing the time allocated for the DL WET and UL WITs. By comparing the maximum sum- versus common-throughput, we characterize the fundamental throughput-fairness trade-offs in a WPCN.

The rest of this paper is organized as follows. Section II presents the WPCN model and the proposed harvest-then-transmit protocol. Section III studies the sum-throughput maximization problem, and characterizes the doubly near-far phenomenon. Section IV formulates the common-throughput maximization problem and presents an efficient algorithm to solve it. Section V presents simulation results on the sum-throughput versus common-throughput comparison. Finally, Section VI concludes the paper.

II. System Model

As shown in Fig. 1, this paper considers a WPCN with WET in the DL and WITs in the UL. The network consists of one H-AP and K users (e.g., sensors) denoted by U_i, $i = 1, \cdots, K$. It is assumed that the H-AP and all user terminals are equipped with one single antenna each. It is further assumed that the H-AP and all the users operate over the same frequency band. In addition, all user terminals are assumed to have no other embedded energy sources; thus, the users need to harvest energy from the received signals broadcast by the H-AP in the DL, which is stored in a rechargeable battery and then used to power operating circuits and transmit information in the UL.

The DL channel from the H-AP to user U_i and the corresponding reversed UL channel are denoted by complex random variables $\tilde{h}_i$ and $\tilde{g}_i$, respectively, with channel power gains $h_i = |\tilde{h}_i|^2$ and $g_i = |\tilde{g}_i|^2$. It is assumed that both the DL and UL channels are quasi-static flat-fading, where h_i's and g_i's remain constant during each block transmission time, denoted by T, but can vary from one block to another. It is further assumed that the H-AP knows both h_i and g_i, $i = 1, \cdots, K$, perfectly at the beginning of each block.

The network adopts a *harvest-then-transmit* protocol as shown in Fig. 2. In each block, the first $\tau_0 T$ amount of time, $0 < \tau_0 < 1$, is assigned to the DL for the H-AP to broadcast wireless energy to all users,

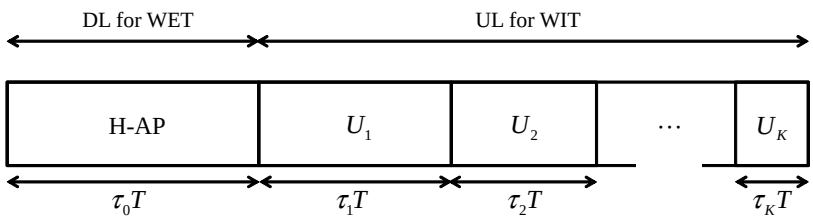

Fig. 2. The harvest-then-transmit protocol.

while the remaining time in the same block is assigned to the UL for information transmissions, during which users transmit their independent information to the H-AP by TDMA. The amount of time assigned to user U_i in the UL is denoted by $\tau_i T$, $0 \leq \tau_i < 1$, $i = 1, \cdots K$. Since τ_0, τ_1, $\cdots$, τ_K represent the time portions in each block allocated to the H-AP and users U_1, $\cdots$, U_K for UL WET and DL WITs, respectively, we have

$$\sum_{i=0}^{K} \tau_i \leq 1. \tag{1}$$

For convenience, we assume a normalized unit block time $T = 1$ in the sequel without loss of generality; hence, we can use both the terms of energy and power interchangeably.

During the DL phase, the transmitted baseband signal of the H-AP in one block of interest is denoted by x_A. We assume that x_A is an arbitrary complex random signal[1] satisfying $\mathbb{E}[|x_A|^2] = P_A$, where P_A denotes the transmit power at the H-AP. The received signal at U_i is then expressed as

$$y_i = \sqrt{h_i} x_A + z_i, \quad i = 1, \ \cdots, \ K, \tag{2}$$

where y_i and z_i denote the received signal and noise at U_i, respectively. It is assumed that P_A is sufficiently large such that the energy harvested due to the receiver noise is negligible. Thus, the amount of energy harvested by each user in the DL can be expressed as (assuming unit block time, i.e., $T = 1$)

$$E_i = \zeta_i P_A h_i \tau_0, \quad i = 1, \ \cdots, \ K, \tag{3}$$

where $0 < \zeta_i < 1$, $i = 1 \ \cdots, \ K$, is the energy harvesting efficiency at each receiver. For convenience, it is assumed that $\zeta_1 = \cdots = \zeta_K = \zeta$ in the sequel of this paper.

After the users replenish their energy during the DL phase, in the subsequent UL phase they transmit independent information to the H-AP in their allocated time slots. It is assumed that at each user terminal,

[1]Note that x_A can also be used to send DL information at the same time; however, this usage will not be considered in this paper. Interested readers may refer to recent works on SWIPT [6]-[11].

a fixed portion of the harvested energy given by (3) is used for its information transmission in the UL, denoted by η_i for U_i, $0 < \eta_i \leq 1$, $i = 1, \cdots, K$. Within τ_i amount of time assigned to U_i, we denote x_i as the complex baseband signal transmitted by U_i, $i = 1, \cdots, K$. We assume Gaussian inputs, i.e., $x_i \sim \mathcal{CN}(0, P_i)$, where $\mathcal{CN}(\mu, \sigma^2)$ stands for a circularly symmetric complex Gaussian (CSCG) random variable with mean μ and variance σ^2, and P_i denotes the average transmit power at U_i, which is given by

$$P_i = \frac{\eta_i E_i}{\tau_i}, \quad i = 1, \cdots, K. \tag{4}$$

For the purpose of exposition, we assume $\eta_i = 1$, $\forall i$, in the sequel, i.e., all the energy harvested at each user is used for its UL information transmission. The received signal at the H-AP in the ith UL slot is then expressed as

$$y_{A,i} = \sqrt{g_i} x_i + z_{A,i}, \quad i = 1, \cdots, K, \tag{5}$$

where $y_{A,i}$ and $z_{A,i}$ denote the received signal and noise at the H-AP, respectively, during slot i. It is assumed that $z_{A,i} \sim \mathcal{CN}(0, \sigma^2)$, $\forall i$. From (3)-(5), the achievable UL throughput of U_i in bits/second/Hz (bps/Hz) can be expressed as

$$\begin{aligned} R_i(\boldsymbol{\tau}) &= \tau_i \log_2\left(1 + \frac{g_i P_i}{\Gamma \sigma^2}\right) \\ &= \tau_i \log_2\left(1 + \gamma_i \frac{\tau_0}{\tau_i}\right), \quad i = 1, \cdots, K, \end{aligned} \tag{6}$$

where $\boldsymbol{\tau} = [\tau_0 \ \tau_1 \ \cdots \tau_K]$, and Γ represents the signal-to-noise ratio (SNR) gap from the additive white Gaussian noise (AWGN) channel capacity due to a practical modulation and coding scheme (MCS) used. In addition, γ_i is given by

$$\gamma_i = \frac{\zeta h_i g_i P_A}{\Gamma \sigma^2}, \quad i = 1, \cdots, K. \tag{7}$$

From (6), it is observed that $R_i(\boldsymbol{\tau})$ increases with τ_0 for a given τ_i. In addition, it can also be shown that $R_i(\boldsymbol{\tau})$ increases with τ_i for a given τ_0. However, τ_0 and τ_i's cannot be increased at the same time given their total time constraint in (1). Fig. 3 shows the throughput given in (6) for the special case of one single user in the network, i.e., $K = 1$, versus the time allocated to the DL WET, τ_0, with $\gamma_1 = 10$dB, assuming that (1) holds with equality, i.e., for the UL WIT $\tau_1 = 1 - \tau_0$. It is observed that the throughput is zero when $\tau_0 = 0$, i.e., no time is assigned for WET to the user in the DL and thus no energy is available for WIT in the UL, as well as when $\tau_0 = 1$ or $\tau_1 = 1 - \tau_0 = 0$, i.e., no time is assigned to the user

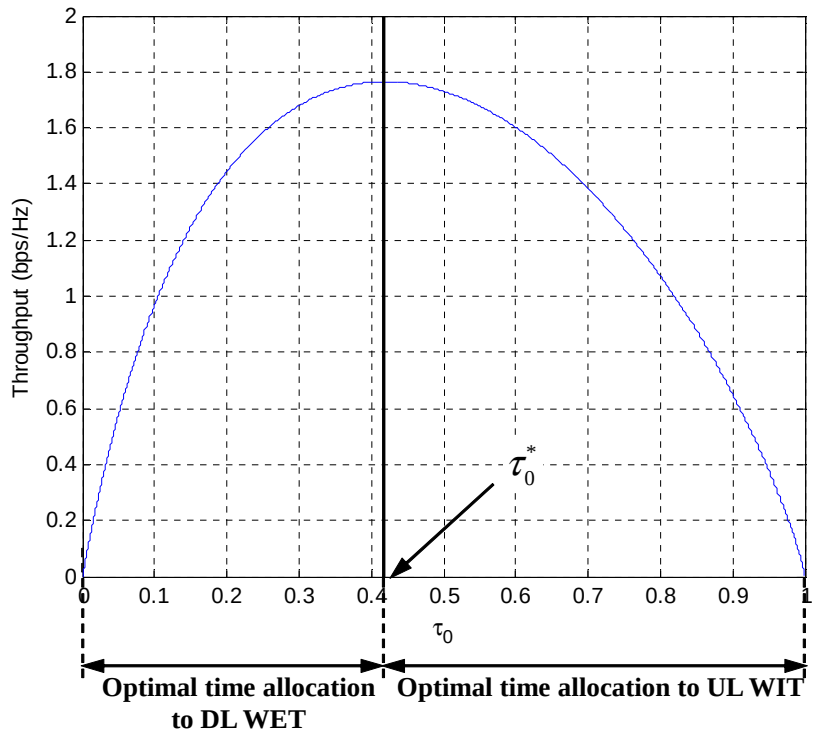

Fig. 3. Throughput versus time allocated to DL WET in a single-user WPCN with $\gamma_1 = 10$dB.

for WIT in the UL. It is also observed that the throughput first increases with τ_0 when $\tau_0 < \tau_0^* = 0.42$, but decreases with increasing τ_0 when $\tau_0 > \tau_0^*$, where τ_0^* is the optimal time allocation to maximize the throughput. This can be explained as follows. With small τ_0, the amount of energy harvested by U_1 in the DL is small. In this regime, as U_1 harvests more energy with increasing τ_0, i.e., more energy is available for the information transmission in the UL, the throughput increases with τ_0. However, as τ_0 becomes larger than τ_0^*, the throughput is decreased more significantly due to the reduction in the allocated UL transmission time, τ_1; as a result, the throughput starts to decrease with increasing τ_0. Therefore, there exists a unique optimal τ_0^* to maximize the throughput.

III. Sum-Throughput Maximization

In this section, we characterize the maximum sum-throughput of the WPCN presented in Section II with arbitrary number of users, K. From (6), the sum-throughput of all users is given by $R_{\text{sum}}(\boldsymbol{\tau}) = \sum_{i=1}^{K} R_i(\boldsymbol{\tau})$, which is a function of the DL and UL time allocation $\boldsymbol{\tau}$. Therefore, from (1) the sum-throughput maximization problem is formulated as

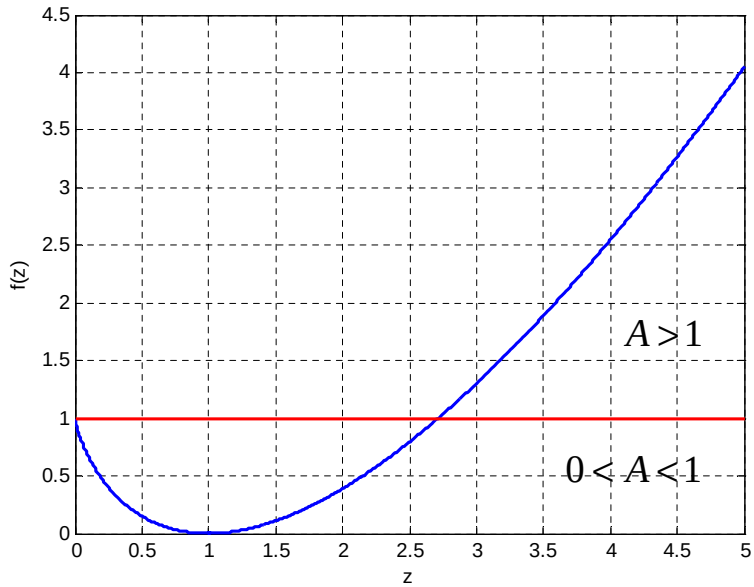

Fig. 4. Plot of $f(z)$ given in (9) versus $z \geq 0$.

$$
\begin{aligned}
(\mathrm{P1}): \quad & \max_{\boldsymbol{\tau}} \quad R_{\mathrm{sum}}(\boldsymbol{\tau}) \\
& \text{s.t.} \quad \sum_{i=0}^{K} \tau_i \leq 1, \\
& \qquad\quad \tau_i \geq 0, \quad i = 0,\ 1,\ \cdots\ K.
\end{aligned} \tag{8}
$$

Lemma 3.1: $R_i(\boldsymbol{\tau})$ is a concave function of $\boldsymbol{\tau}$ for any given $i \in \{1,\ \cdots,\ K\}$.

Proof: Please refer to Appendix A. ■

From Lemma 3.1, it follows that $R_{\mathrm{sum}}(\boldsymbol{\tau})$ is also a concave function of $\boldsymbol{\tau}$ since it is the summation of $R_i(\boldsymbol{\tau})$'s. Therefore, $(\mathrm{P1})$ is a convex optimization problem, and thus can be solved by convex optimization techniques. To solve $(\mathrm{P1})$, we first have the following lemma.

Lemma 3.2: Given $A > 0$, there exists a unique $z^* > 1$ that is the solution of $f(z) = A$, where

$$
f(z) \triangleq z \ln z - z + 1, \quad z \geq 0. \tag{9}
$$

Proof: Please refer to Appendix B. ■

Fig. 4 shows $f(z)$ given in (9) with $z \geq 0$. It is observed that $f(z)$ is a convex function over $z \geq 0$ where the minimum is attained at $z = 1$ with $f(1) = 0$. Therefore, given $0 < A \leq 1$, there are two different solutions for $f(z) = A$, among which one is smaller than 1 and the other is larger than 1, i.e.,

$z^* > 1$. On the other hand, if $A > 1$, there is only one solution for $f(z) = A$, which is larger than 1, i.e., $z^* > 1$. The above observations are thus in accordance with Lemma 3.2.

Proposition 3.1: The optimal time allocation solution for $(\mathrm{P1})$, denoted by $\boldsymbol{\tau}^* = [\tau_0^* \ \tau_1^* \ \cdots \ \tau_K^*]$, is given by

$$\tau_i^* = \begin{cases} \frac{z^*-1}{A+z^*-1} & , \quad i = 0 \\ \frac{\gamma_i}{A+z^*-1} & , \quad i = 1, \cdots, K \end{cases} \tag{10}$$

where $A \triangleq \sum_{i=1}^{K} \gamma_i > 0$ and $z^* > 1$ is the corresponding solution of $f(z) = A$ as given by Lemma 3.2.

Proof: Please refer to Appendix C. ■

It is worth noting that $A > 0$ always holds since from (7) we have $\gamma_i > 0$, $i = 1, \ 2, \ \cdots, K$, provided that $h_i \neq 0$ and $g_i \neq 0$. Hence, given a set of strictly positive γ_i's, according to Lemma 3.2 $z^* > 1$ is uniquely determined with the presumed A, thus resulting in a unique solution $\boldsymbol{\tau}^*$ for $(\mathrm{P1})$, with $\tau_i^* > 0$, $i = 0, \ 1, \ \cdots, \ K$, i.e., the time allocated to the DL WET is always greater than zero, and so is the time allocated to each user in the UL WIT, provided that $\gamma_i > 0$, $\forall i$. Furthermore, from Proposition 3.1 we have the following corollary.

Corollary 3.1: In the optimal time allocation solution of $(\mathrm{P1})$, τ_0^* is a monotonically decreasing function of $A > 0$.

Proof: Please refer to Appendix D. ■

From Corollary 3.1, it is inferred that the time allocated to the DL WET decreases with increasing γ_i's, or channel power gains h_i's and/or g_i's, since $A = \sum_{i=1}^{K} \gamma_i$ and $\gamma_i \propto h_i g_i$, $i = 1, \ \cdots, K$, as shown in (7). As a result, τ_i^*'s, $i = 1, \ \cdots, \ K$, increase with A, i.e., the time allocated to the UL WIT increases with γ_i's. This is an interesting observation implying that when the channel power gains, h_i's and g_i's, become larger, we should allocate more time to the UL WITs instead of the DL WET to maximize the sum-throughput. This is because with larger γ_i's, the required energy for UL WITs becomes smaller given any transmission rate; thus, each user can harvest sufficient amount of wireless energy from the H-AP even with a smaller time allocated to the DL WET.

Note that the sum-throughput maximization solution given in (10) allocates more time to a 'near' user to the H-AP than a 'far' user, since in practice $h_i \propto D_i^{-\alpha_d}$, $g_i \propto D_i^{-\alpha_u}$, and $\gamma_i \propto h_i g_i$ according to (7), where $\alpha_d \geq 2$ and $\alpha_u \geq 2$ denote the channel pathloss exponents in the DL and UL, respectively, and D_i denotes the distance between the H-AP and U_i. Thus, from (10) it follows that $\tau_i^* \propto D_i^{-(\alpha_d+\alpha_u)}$,

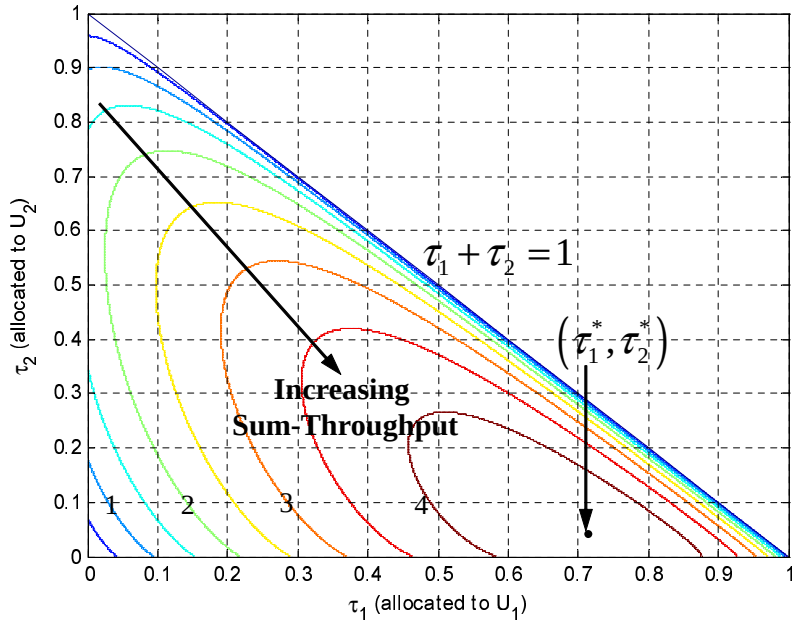

Fig. 5. Sum-throughput (in bps/Hz) versus time allocation.

$i = 1, \cdots, K$, which results in an unfair time and throughput allocation among users in the WPCN, a phenomenon termed "doubly near-far problem". To further illustrate this issue, Fig. 5 shows the sum-throughput $R_{\text{sum}}(\boldsymbol{\tau})$ versus UL WIT time allocation τ_1 and τ_2 for a two-user network with $K = 2$ and $D_1 = \frac{1}{2}D_2$. It is assumed that the channel reciprocity holds for the DL and UL and thus $h_i = g_i$, $i = 1, 2$, with $\alpha_d = \alpha_u = 2$. Accordingly, we set $\gamma_1 = 22$dB and $\gamma_2 = 10$dB, with $\gamma_1/\gamma_2 = (D_2/D_1)^{\alpha_d+\alpha_u}$. It is observed from Fig. 5 that $R_{\text{sum}}(\boldsymbol{\tau}) = 0$ when $\tau_1 = \tau_2 = 0$, $\tau_0 = 1 - (\tau_1 + \tau_2) = 1$, or $\tau_1 + \tau_2 = 1$, $\tau_0 = 0$, since no time is allocated to the users for the UL WITs in the former case, while no time is allocated to the DL WET in the latter case. The numerical result of sum-throughput clearly shows that $R_{\text{sum}}(\boldsymbol{\tau})$ is strictly positive when $0 < \tau_1 + \tau_2 < 1$. In addition, it is observed that the optimal DL and UL time allocation to maximize the sum-throughput is $\boldsymbol{\tau}^* = [0.2441,\ 0.7114,\ 0.0445]$ where $\tau_1^* = 16\tau_2^*$, i.e., $\tau_1^* = (D_2/D_1)^{\alpha_d+\alpha_u}\tau_2^*$, which is consistent with (10). Furthermore, at the optimal $\boldsymbol{\tau}^*$, $R_{\text{sum}}(\boldsymbol{\tau}^*) = 4.58$ bps/Hz, with $R_1(\boldsymbol{\tau}^*) = 4.13$ bps/Hz and $R_2(\boldsymbol{\tau}^*) = 0.45$ bps/Hz, which demonstrates the very unfair throughput allocation between the two users due to the doubly near-far problem.

For comparison, we consider UL transmissions in a conventional TDMA-based wireless network with WIT only [13]-[16], where each user is equipped with a constant energy supply, and thus has an equal energy consumption at each block denoted by $\bar{E}$. It then follows from (7) that $\gamma_i \propto D_i^{-\alpha_u}$ and thus from

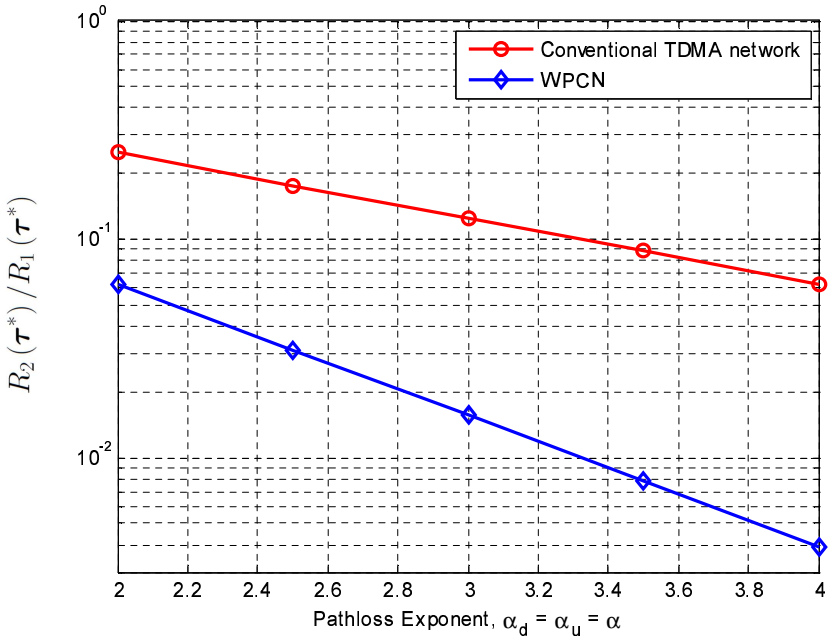

Fig. 6. Throughput ratio in a two-user WPCN versus conventional TDMA network with equal energy supply.

(10), the optimal time allocation to maximize the sum-throughput of such a conventional TDMA network should satisfy $\tau_i^* \propto D_i^{-\alpha_u}$, $i = 1, \cdots, K$, and $\tau_0^* = 0$ (since no DL WET is needed). Clearly, the WPCN suffers from a more severe near-far problem than the conventional TDMA network. With the same setup as for Fig. 5, in Fig. 6 we show the optimal throughput of U_2, $R_2(\boldsymbol{\tau}^*)$, normalized by that of U_1, $R_1(\boldsymbol{\tau}^*)$, in a WPCN versus that in a conventional TDMA network for different values of the pathloss exponent α, with $\alpha_d = \alpha_u = \alpha$. For the WPCN, γ_1 is set to be fixed as $\gamma_1 = 22$dB for U_1, while $\gamma_2 = 10$, 7, 4, 1, and -2dB for $\alpha = 2$, 2.5, 3, 3.5, and 4, respectively, since $\gamma_1/\gamma_2 = (D_2/D_1)^{2\alpha}$. For the conventional TDMA network, $\bar{E}$ for both U_1 and U_2 are assumed to be $\bar{E} = \frac{1}{2}(E_1 + E_2)$ with E_1 and E_2 denoting the average harvested energy at U_1 and U_2 in the WPCN under comparison, respectively; it then follows that for the conventional TDMA network, $\gamma_1 = 13$dB and $\gamma_2 = 7.1$, 5.5, 4.0, 2.4, and 0.9dB for $\alpha = 2$, 2.5, 3, 3.5, and 4, respectively. From Fig. 6, it is observed that the throughput ratio of the two users in the WPNC case decreases twice faster than that in the conventional TDMA in the logarithm scale due to the more severe (doubly) near-far problem.

IV. Common-Throughput Maximization

In this section, we tackle the doubly near-far problem in the WPNC by applying the common-throughput maximization approach, which guarantees equal throughput allocations to all users and yet maximize their

sum-throughput. From (1) and (6), the common-throughput maximization problem is formulated as

$$\begin{aligned} (\mathrm{P2}): \ \max_{\bar{R},\boldsymbol{\tau}} \ & \bar{R} \\ \text{s.t.} \ & R_i(\boldsymbol{\tau}) \geq \bar{R}, \ \ i = 1 \cdots K, \\ & \boldsymbol{\tau} \in \mathcal{D}, \end{aligned} \tag{11}$$

where $\bar{R}$ denotes the common-throughput and $\mathcal{D}$ is the feasible set of $\boldsymbol{\tau}$ specified by (1) and (8).

Remark 4.1: Problem $(\mathrm{P2})$ is designed to guarantee the throughput of the user with the worst channel condition, e.g., of the largest distance from the H-AP. Since $R_i(\boldsymbol{\tau})$ given by (6) is a monotonically increasing function of both τ_0 and τ_i, it can be easily shown that the optimal time allocation solution $\boldsymbol{\tau}^*$ for $(\mathrm{P2})$ should allocate the same optimal throughput to all the users, denoted by $\bar{R}^* = R_1(\boldsymbol{\tau}^*) = \cdots = R_K(\boldsymbol{\tau}^*)$, with $\sum_{i=0}^{K} \tau_i^* = 1$, when the minimum user throughput in the network is maximized. In addition, allocating equal throughput to all users can be relevant in practice, since one typical application of the WPCN is sensor network, where all the sensors may need to periodically send their sensing data to a function center (modelled as the H-AP in our setup) with the same rate.

The maximum common-throughput $\bar{R}^*$ is the maximum of all the feasible common-throughput $\bar{R}$ that satisfies the rate inequalities in (11) of $(\mathrm{P2})$. To solve $(\mathrm{P2})$, given any $\bar{R} > 0$, we first consider the following feasibility problem:

$$\begin{aligned} \text{Find} \ & \boldsymbol{\tau} \\ \text{s.t.} \ & R_i(\boldsymbol{\tau}) \geq \bar{R}, \ \ i = 1, \ \cdots, K, \\ & \boldsymbol{\tau} \in \mathcal{D}. \end{aligned} \tag{12}$$

Since the problem in (12) is convex, we consider its Lagrangian given by

$$\mathcal{L}(\boldsymbol{\tau}, \boldsymbol{\lambda}) = -\sum_{i=1}^{K} \lambda_i \left(R_i(\boldsymbol{\tau}) - \bar{R}\right), \tag{13}$$

where $\boldsymbol{\lambda} = [\lambda_1, \ \cdots, \lambda_K] \geq 0$ ('$\geq$' denotes the component-wise inequality) consists of the Lagrange multipliers associated with the K user throughput constraints in problem (12). The dual function of problem (12) is then given by

$$\mathcal{G}(\boldsymbol{\lambda}) = \min_{\boldsymbol{\tau} \in \mathcal{D}} \mathcal{L}(\boldsymbol{\tau}, \boldsymbol{\lambda}). \tag{14}$$

The dual function $\mathcal{G}(\boldsymbol{\lambda})$ can be used to determine whether problem (12) is feasible, as provided in the following lemma.

Lemma 4.1: For a given $\bar{R} > 0$, problem (12) is infeasible if and only if there exists an $\boldsymbol{\lambda} \geq 0$ such that $\mathcal{G}(\boldsymbol{\lambda}) > 0$.

Proof: Please refer to Appendix E. ■

Next, we obtain $\mathcal{G}(\boldsymbol{\lambda})$ in (14) for a given $\boldsymbol{\lambda} \geq 0$ by solving the following weighted sum-throughput maximization problem, which follows from (13).

$$\begin{aligned} \max_{\boldsymbol{\tau}} \quad & \sum_{i=1}^{K} \lambda_i R_i(\boldsymbol{\tau}) \\ \text{s.t.} \quad & \boldsymbol{\tau} \in \mathcal{D}. \end{aligned} \tag{15}$$

Like (P1), the problem in (15) is convex and thus can be solved by convex optimization techniques. Similar to Proposition 3.1 for the sum-throughput maximization case with $\lambda_i = 1$, $\forall i$, we obtain the optimal time allocation solution for the weighted sum-throughput maximization problem in (15), given in the following proposition.

Proposition 4.1: Given $\boldsymbol{\lambda} \geq 0$, the optimal time allocation solution for (15), denoted by $\boldsymbol{\tau}^\star = [\tau_0^\star,\ \tau_1^\star,\ \cdots, \tau_K^\star]$, is

$$\tau_0^\star = \frac{1}{1 + \sum\limits_{j=1}^{K} \left(\gamma_j / z_j^\star\right)}, \tag{16}$$

$$\tau_i^\star = \frac{\gamma_i / z_i^\star}{1 + \sum\limits_{j=1}^{K} \left(\gamma_j / z_j^\star\right)}, \quad i = 1,\ \cdots,\ K, \tag{17}$$

where $z_i^\star$, $i = 1,\ \cdots,\ K$, is the solution of the following equations:

$$\ln(1 + z_i) - \frac{z_i}{1 + z_i} = \frac{\mu^\star}{\lambda_i} \ln 2, \tag{18}$$

$$\sum_{i=1}^{K} \frac{\lambda_i \gamma_i}{1 + z_i} = \mu^\star \ln 2, \tag{19}$$

with $\mu^\star > 0$ being a constant.

Proof: Please refer to Appendix F. ■

With Proposition 4.1, we can compute $\boldsymbol{\tau}^\star$ efficiently as follows. Denote the left-hand sides (LHSs) of (18) and (19) as $Q(z_i)$ and $S(\mathbf{z})$ with $\mathbf{z} = [z_1,\ z_2,\ \cdots,\ z_K]$, respectively. Note that $Q(z_i)$ is an increasing function of z_i, $i = 1,\ \cdots, K$ (see Appendix C), whereas $S(\mathbf{z})$ is a decreasing function with respect to

TABLE I

ALGORITHM TO SOLVE (P2).

1) **Initialize** $R_{\min} = 0$, $R_{\max} > \bar{R}^*$.[2]

2) **Repeat**

1. $\bar{R} = \frac{1}{2}(R_{\min} + R_{\max})$.
2. Initialize $\boldsymbol{\lambda} \geq 0$.
3. Given $\boldsymbol{\lambda}$, solve the problem in (15) by Proposition 4.1.
4. Compute $\mathcal{G}(\boldsymbol{\lambda})$ using (13).
5. If $\mathcal{G}(\boldsymbol{\lambda}) > 0$, $\bar{R}$ is infeasible, set $R_{\max} \leftarrow \bar{R}$, go to step 1. Otherwise, update $\boldsymbol{\lambda}$ using the ellipsoid method and the subgradient of $\mathcal{G}(\boldsymbol{\lambda})$ given by (20). If the stopping criteria of the ellipsoid method is not met, go to step 3.
6. Set $R_{\min} \leftarrow \bar{R}$.

3) **Until** $R_{\max} - R_{\min} < \delta$, where $\delta > 0$ is a given error tolerance.

each individual z_i. Given any $\mu > 0$, suppose that z_i is the solution of $Q(z_i) = \frac{\mu}{\lambda_i}\ln 2$, $i = 1, \cdots, K$, in (18). With these z_i's, there are two possible cases to consider next. If in (19) the resulting $S(\mathbf{z}) > \mu \ln 2$, we should increase μ since z_i's satisfying $Q(z_i) = \frac{\mu}{\lambda_i}\ln 2$, $i = 1, \cdots, K$, will increase with μ given that $Q(z_i)$, $\forall i$, is an increasing function of z_i; as a result, $S(\mathbf{z})$ will decrease since it is a decreasing function of each individual z_i. Otherwise, μ should be decreased to satisfy (19) if $S(\mathbf{z}) < \mu \ln 2$. Therefore, $z_i^\star$'s and $\mu^\star$ can be obtained by iteratively updating z_i's and μ as above until convergence is reached. Then, $\boldsymbol{\tau}^\star$ can be computed from (16) and (17) accordingly.

Given $\bar{R}$, $\boldsymbol{\lambda}$, and the obtained $\boldsymbol{\tau}^\star$ by solving problem (15) with Proposition 4.1, we can compute the corresponding $R_i(\boldsymbol{\tau}^\star)$, $i = 1, \cdots, K$, and thus $\mathcal{G}(\boldsymbol{\lambda})$ in (14) using (13). If $\mathcal{G}(\boldsymbol{\lambda}) > 0$, it follows from Lemma 4.1 that problem (12) is infeasible, i.e., $\bar{R} > \bar{R}^*$. Therefore, we should decrease $\bar{R}$ and solve the feasibility problem in (12) again. On the other hand, if $\mathcal{G}(\boldsymbol{\lambda}) \leq 0$, we can update $\boldsymbol{\lambda}$ using sub-gradient based algorithms, e.g. the ellipsoid method [17], with the subgradient of $\mathcal{G}(\boldsymbol{\lambda})$, denoted by $\boldsymbol{\upsilon} = [\upsilon_1 \ \ \upsilon_2 \ \ \cdots \ \ \upsilon_K]^T$, given by

$$\upsilon_i = \tau_i^\star \log_2\left(1 + \frac{\gamma_i \tau_0^\star}{\tau_i^\star}\right) - \bar{R}, \ \ 1 \leq i \leq K, \tag{20}$$

until $\boldsymbol{\lambda}$ converges to $\boldsymbol{\lambda}^*$ with $\boldsymbol{\lambda}^*$ denoting the maximizer of $\mathcal{G}(\boldsymbol{\lambda})$ or the optimal dual solution for problem (12). If $\mathcal{G}(\boldsymbol{\lambda}^*) \leq 0$, it then follows that problem (12) is feasible and thus $\bar{R} \leq \bar{R}^*$. In this case, $\bar{R}$ should be increased for solving the feasibility problem in (12) again. Consequently, $\bar{R}^*$ can be obtained numerically

[2]The initial value of $R_{\max}$ can be chosen as any arbitrary large number such that it satisfies $R_{\max} > \bar{R}^*$.

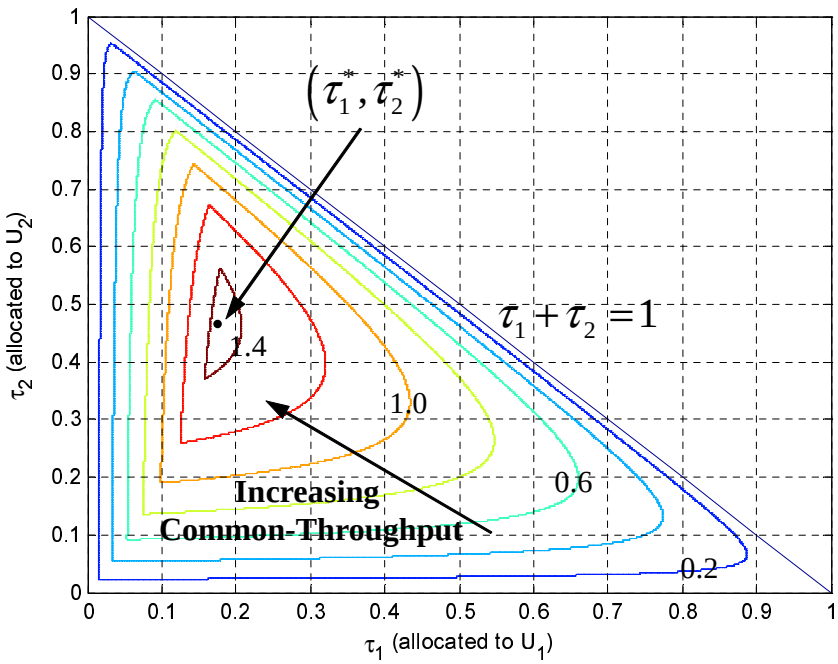

Fig. 7. Common-throughput (in bps/Hz) versus time allocation.

by iteratively updating $\bar{R}$ by a simple bisection search [12]. To summarize, one algorithm to solve $(\mathrm{P2})$ is given in Table I.[3]

Fig. 7 shows the common-throughput in bps/Hz versus τ_1 and τ_2 for the same two-user channel setup as for Fig. 5. It is observed that the optimal time allocation for (P2) is given by $\boldsymbol{\tau}^* = [0.3683, \quad 0.1386, \quad 0.4932]$, which results in $\bar{R}^* = R_1(\boldsymbol{\tau}^*) = R_2(\boldsymbol{\tau}^*) = 1.46$bps/Hz. Comparing to Fig. 5 where the sum-throughput is maximized, the time portion allocated to the near user, U_1, is decreased substantially from 0.7114 to 0.1737, while that to the far user, U_2, is greatly increased from 0.0445 to 0.4669. Consequently, the throughput of U_2 is increased from 0.45bps/Hz to 1.46bps/Hz, while that of U_1 is decreased from 4.13bps/Hz to 1.46bps/Hz, the same throughput as U_2. This result shows the effectiveness of the proposed common-throughput approach for tackling the doubly near-far problem in a WPCN.

Fig. 8 shows the ratio of the optimal time allocated to the far user U_2 over that to the near user U_1, i.e., τ_2^*/τ_1^*, in $(\mathrm{P1})$ versus $(\mathrm{P2})$, with different values of the common pathloss exponent α in both DL and UL, where the same two-user channel setup as for Fig. 5 is considered. It is assumed that γ_1 for the near user U_1 is fixed as $\gamma_1 = 22$dB and γ_2 for the far user U_2 is set the same as for Fig. 6. It is observed that the

[3]The computational complexity of the proposed algorithm in Table I can be shown to be $\mathcal{O}(K^3)$ since at each iteration it performs K one-dimension searches each with the complexity of $\mathcal{O}(1)$ to find $\boldsymbol{\tau}^\star$, and the ellipsoid method has the complexity of $\mathcal{O}(K^2)$ [17] to converge.

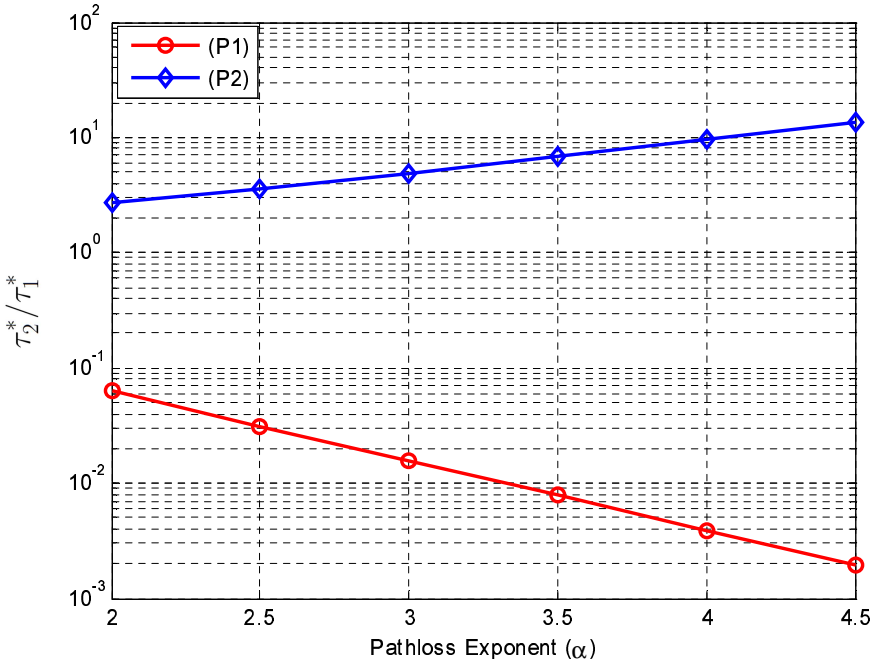

Fig. 8. Comparison of the ratio of time allocated to U_2 and $U1$ in (P1) versus (P2).

time ratio of (P1) in the logarithm scale decreases linearly with α to maximize the sum-throughput, which can also be inferred from (10), due to the doubly near-far problem. On the contrary, τ_2^*/τ_1^* is observed to increase with α to maximize the common-throughput in (P2), since more time is allocated to the far user U_2 instead of the near user U_1 as the ratio between γ_1 and γ_2, i.e., γ_1/γ_2, increases with α.

Notice that (P1) and (P2) deal with two extreme cases of throughput allocation to the users in a WPNC where the fairness is completely ignored and a strict equal fairness is imposed, respectively. More generally, Fig. 9 shows the achievable throughput region of a two-user WPCN by solving the weighted sum-throughput maximization problem in (15) with different throughput weights for the near and far users, under the same channel setup as for Fig. 5. It is observed that the boundary of the throughput region characterizes all the optimal throughput-fairness trade-offs in this two-user WPCN, which include the throughput pairs obtained by solving (P1) for the maximum sum-throughput and by solving (P2) for the maximum common-throughput, shown as points (a) and (b) in the figure, respectively.

Remark 4.2: It is worth noting that the common-throughput approach for characterizing the achievable rate region of multi-user communication systems under strict fairness constraints can be considered as one special case of the "rate-profile" method proposed in [18]. Hence, the common-throughput approach investigated in this paper can be easily extended to the general case where the required throughput of

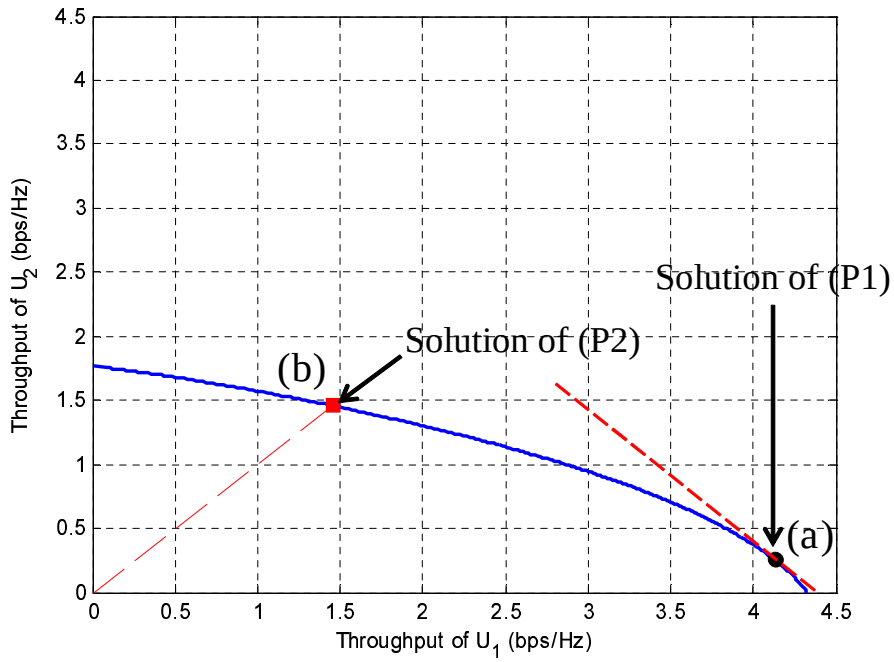

Fig. 9. Throughput region of a two-user WPCN with (a) corresponding to the maximum sum-throughput; and (b) corresponding to the maximum common-throughput.

each user is different using the rate-profile method. Given $\bar{\mathbf{R}} = \left[\bar{R}_1 \ \bar{R}_2 \ \cdots \ \bar{R}_K\right]$ with $\bar{R}_i$ denoting the required throughput of user i, $i = 1, \cdots, K$, the corresponding rate profile vector is defined as $\boldsymbol{\beta} = [\beta_1 \ \beta_2 \ \cdots \ \beta_K]$ where $\beta_i = \bar{R}_i / \sum_{j=1}^{K} \bar{R}_j$ (Note that the common-throughput maximization problem (P2) is thus for a special case with $\beta_i = 1/K, \forall i$). The optimal time allocation solution to maximize the system sum-throughput subject to the rate fairness constraint with any given $\boldsymbol{\beta}$ can be obtained using the same algorithm proposed for (P2) in this paper, with the throughput constraint in (11) replaced by $R_i(\tau) \geq \beta_i \bar{R}$, $i = 1, \cdots, K$, where $\bar{R}$ here denotes the sum-throughput of all users.

V. Simulation Result

In this section, we compare the maximum sum-throughput by (P1) versus the maximum common-throughput by (P2) in an example WPCN. The bandwidth is set as 1MHz. It is assumed that the channel reciprocity holds for the DL and UL and thus $h_i = g_i$, $i = 1, \cdots, K$, with the same pathloss exponent $\alpha_d = \alpha_u = \alpha$. Accordingly, both the DL and UL channel power gains are modeled as $h_i = g_i = 10^{-3} \rho_i^2 D_i^{-\alpha}$, $i = 1, \cdots, K$, where ρ_i represents the additional channel short-term fading which is assumed to be Rayleigh distributed, and thus ρ_i^2 is an exponentially distributed random variable with unit mean. Note that in the above channel model, a 30dB average signal power attenuation is assumed at a reference

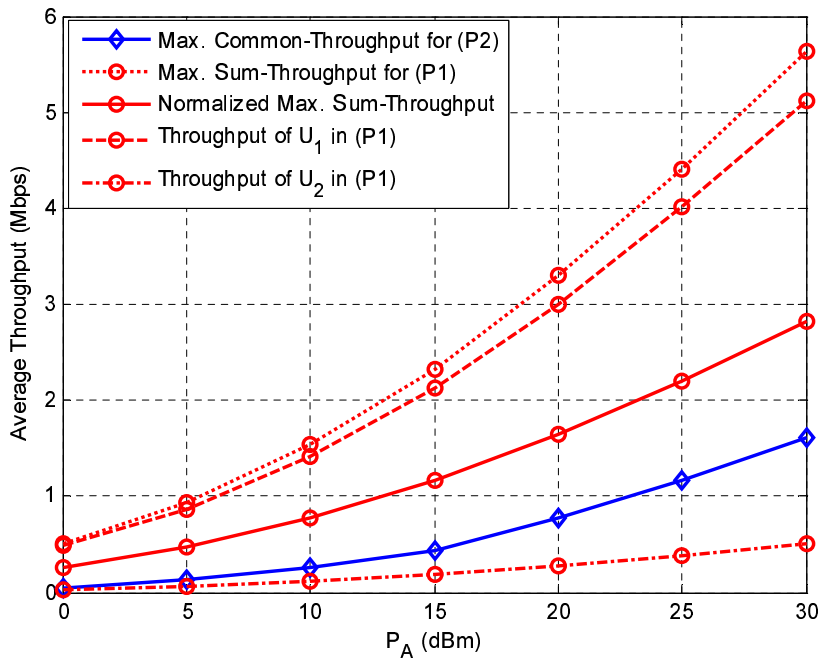

Fig. 10. Sum-throughput vs. common-throughput.

distance of 1m. The AWGN at the H-AP receiver is assumed to have a white power spectral density of -160dBm/Hz. For each user, the energy harvesting efficiency for WET is assumed to be $\zeta = 0.5$. Finally, we set $\Gamma = 9.8$dB assuming that an uncoded quadrature amplitude modulation (QAM) is employed [19].

Fig. 10 shows the maximum sum-throughput versus the maximum common-throughput in the same WPCN with $K = 2$, $D_1 = 5$m, and $D_2 = 10$m for different values of transmit power at H-AP, P_A, in dBm, by averaging over 1000 randomly generated fading channel realizations, with fixed $\alpha = 2$. As shown in Fig. 10, when the sum-throughput is maximized, the throughput of U_1 dominates over that of U_2 due to the doubly near-far problem, which results in notably unfair rate allocation between the near user (U_1) and far user (U_2) in this example. It is also observed that the maximum common-throughput for the two users is smaller than the normalized maximum sum-throughput by the number of users, i.e., $R_{\text{sum}}(\boldsymbol{\tau})/K$ ($K = 2$ in this example), which is a cost to pay in order to ensure a strictly fair rate allocation to the two users regardless of their distances from the H-AP.

Next, by fixing $P_A = 20$dBm, Fig. 11 shows the throughput comparison for different values of the common pathloss exponent α in both the DL and UL in the same WPCN as for Fig. 10. It is observed that when the sum-throughput is maximized, the throughput of the near user U_1 converges to the maximum sum-throughput as α increases, whereas that of the far user U_2 converges to zero, which indicates that the

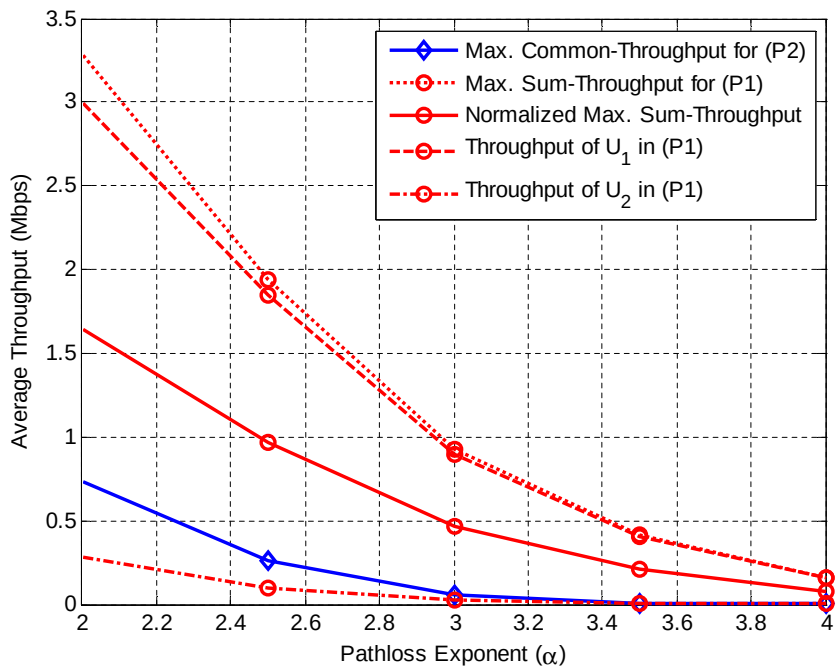

Fig. 11. Throughput vs. pathloss exponent.

WPCN suffers from a more severe unfair rate allocation between the near and far users as the pathloss exponent increases, due to the doubly near-far problem. In addition, the maximum common-throughput for the two users is observed to decrease faster with increasing α than the normalized maximum sum-throughput. This is because as α increases, (P2) allocates more time to the far user U_2 instead of near user U_1 in order to ensure the equal throughput allocation among users since the ratio γ_1/γ_2 increases with α, whereas (P1) allocates more time to U_1 instead of U_2 as α increases.

At last, Fig. 12 shows the throughput over number of users, K. It is assumed that K users in the network are equally separated from the H-AP according to $D_i = \frac{D_K}{K} \times i$, $i = 1, \cdots K$, where $D_K = 10$m. The transmit power at the H-AP and the pathloss exponent are set to be fixed as $P_A = 20$dBm and $\alpha = 2$, respectively. In addition, we compare with the throughput achievable by equal time allocation (ETA), i.e., $\tau_i = \frac{1}{K+1}$, $i = 0, \cdots, K$, as a low-complexity time allocation scheme. It is observed that both the normalized maximum sum-throughput by solving (P1) and the maximum common-throughput by solving (P2) decreases with increasing K, and they outperform the sum-throughput and the minimum throughput (over all users) by the heuristic ETA scheme, respectively.

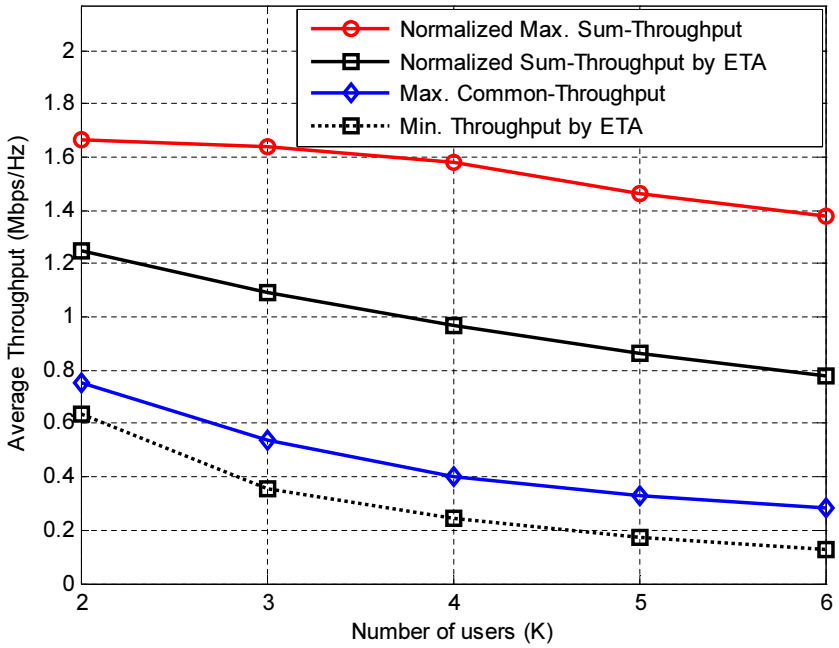

Fig. 12. Throughput vs. number of users (K).

VI. Conclusion

This paper has studied a new type of wireless RF (radio frequency) powered communication network with a harvest-then-transmit protocol, where the H-AP first broadcasts wireless energy to distributed users in the downlink and then the users transmit their independent information to the H-AP in the uplink by TDMA. Our results reveal an interesting new phenomenon in such hybrid energy-information transmission networks, so-called doubly near-far problem, which is due to the folded signal attenuation in both the downlink WET and uplink WIT. As a result, notably unfair time and throughput allocation among the users occurs when the conventional metric of network sum-throughput is maximized. To overcome this problem, we propose a new common-throughput maximization approach to allocate equal rates to all users regardless of their distances from the H-AP by allocating the transmission time to users inversely proportional to their distances to the H-AP. Simulation results showed that this approach is effective in solving the doubly near-far problem in the WPCN, but at a cost of sum-throughput degradation.

APPENDIX A
PROOF OF LEMMA 3.1

Denote the Hessian of $R_i(\boldsymbol{\tau})$ defined in (6) as

$$\nabla^2 R_i(\boldsymbol{\tau}) = \left[d_{j,m}^{(i)}\right], \ \ 0 \le j, m \le K,$$

where $d_{j,m}^{(i)}$ denotes the element of $\nabla^2 R_i(\boldsymbol{\tau})$ at the jth row and mth column. From (6), the diagonal entries of $\nabla^2 R_i(\boldsymbol{\tau})$, i.e., $j = m$, can be expressed as

$$d_{j,j}^{(i)} = \begin{cases} -\frac{1}{\ln 2}\gamma_i^2 \tau_i^{-1} \beta_i^{-2} & , \quad j = 0 \\ -\frac{1}{\ln 2}\gamma_i^2 \tau_0^2 \tau_i^{-3} \beta_i^{-2} & , \quad j = i \\ 0 & , \ \text{otherwise}, \end{cases} \tag{21}$$

where $\beta_i = 1 + \frac{\gamma_i \tau_0}{\tau_i}$. In addition, the off-diagonal entries of $\nabla^2 R_i(\boldsymbol{\tau})$ can be expressed as

$$d_{j,m}^{(i)} = d_{m,j}^{(i)} = \begin{cases} \frac{1}{\ln 2}\gamma_i^2 \tau_0 \tau_i^{-2} \beta_i^{-2} & , \ j = i \ \text{and} \ m = 0 \\ 0 & , \quad \text{otherwise}. \end{cases} \tag{22}$$

Given an arbitrary real vector $\mathbf{v} = [v_0, \ v_1, \ \cdots, \ v_K]^T$, since $\tau_i \ge 0$, it can be shown from (21) and (22) that

$$\begin{aligned} \mathbf{v}^T \nabla^2 R_i(\boldsymbol{\tau}) \mathbf{v} &= -\frac{1}{\ln 2}\frac{1}{\beta_i^2}\frac{\gamma_i^2}{\tau_i^3}(v_i \tau_0 - v_0 \tau_i)^2 \\ &\le 0, \end{aligned}$$

i.e., $\nabla^2 R_i(\boldsymbol{\tau})$, $\forall i$, is a negative semidefinite matrix. Therefore, $R_i(\boldsymbol{\tau})$ is a concave function of $\boldsymbol{\tau} = [\tau_0 \ \ \tau_1 \ \ \cdots \ \ \tau_N]^T$ [12]. This completes the proof of Lemma 3.1.

APPENDIX B
PROOF OF LEMMA 3.2

From (9), we have

$$\lim_{z \to 0} f(z) = 1, \tag{23}$$

$$\frac{\partial f(z)}{\partial z} = \ln z, \tag{24}$$

$$\frac{\partial^2 f(z)}{\partial z^2} = \frac{1}{z}. \tag{25}$$

Thus it follows from (24) and (25) that $f(z)$ is a convex function over $z \ge 0$ and its minimum is attained at $z = 1$ with $f(1) = 0$. This implies that $f(z) \ge 0$ with $z \ge 1$ and is monotonically increasing with z in this regime. Therefore, given $A > 0$, $f(z) = A$ has a unique solution $z^* > 1$. This completes the proof of Lemma 3.2.

APPENDIX C
PROOF OF PROPOSITION 3.1

The Lagrangian of $(\mathrm{P1})$ is given by

$$\mathcal{L}_{\mathrm{sum}}\left(\boldsymbol{\tau},\nu\right)=R_{\mathrm{sum}}\left(\boldsymbol{\tau}\right)-\nu\left(\sum_{i=0}^{K}\tau_i-1\right), \tag{26}$$

where $\nu\geq 0$ denotes the Lagrange multiplier associated with the constraint in (1). The dual function of $(\mathrm{P1})$ is thus given by

$$\mathcal{G}\left(\nu\right)=\min_{\boldsymbol{\tau}\in\mathcal{D}}\ \mathcal{L}_{\mathrm{sum}}\left(\boldsymbol{\tau},\nu\right), \tag{27}$$

where $\mathcal{D}$ is the feasible set of $\boldsymbol{\tau}$ specified by (1) and (8).

It can be shown from (1) and (8) that there exists an $\boldsymbol{\tau}\in\mathcal{D}$ with $\tau_i>0$, $i=0,\ 1,\ \cdots\ K$, satisfying $\sum\limits_{i=0}^{K}\tau_i<1$, and thus strong duality holds for this problem thanks to the Slater's condition [12]. Since $(\mathrm{P1})$ is a convex optimization problem for which the strong duality holds, the Karush-Kuhn-Tucker (KKT) conditions are both necessary and sufficient for the global optimality of $(\mathrm{P1})$, which are given by

$$\sum_{i=0}^{K}\tau_i^*\leq 1, \tag{28}$$

$$\nu^*\left(\sum_{i=0}^{K}\tau_i^*-1\right)=0, \tag{29}$$

$$\frac{\partial}{\partial\tau_i}R_{\mathrm{sum}}\left(\boldsymbol{\tau}^*\right)-\nu^*=0,\quad i=0,\ \cdots,\ K, \tag{30}$$

where τ_i^*'s and ν^* denote the optimal primal and dual solutions of $(\mathrm{P1})$, respectively. It can be easily verified that $\sum\limits_{i=0}^{K}\tau_i^*=1$ must hold for $(\mathrm{P1})$ and thus from (29) without loss of generality, we assume $\nu^*>0$. From (30), it follows that

$$\sum_{i=1}^{K}\frac{\gamma_i}{1+\gamma_i\frac{\tau_0^*}{\tau_i^*}}=\nu^*\ln 2, \tag{31}$$

$$t\left(\gamma_i\frac{\tau_0^*}{\tau_i^*}\right)=\nu^*\ln 2,\quad 1\leq i\leq K, \tag{32}$$

where $t\left(x\right)$ is defined as

$$t\left(x\right)\triangleq\ln\left(1+x\right)-\frac{x}{1+x},\quad x\geq 0. \tag{33}$$

Given $1\leq i,j\leq K$, from (31) we have

$$t\left(\gamma_i\frac{\tau_0^*}{\tau_i^*}\right)=t\left(\gamma_j\frac{\tau_0^*}{\tau_j^*}\right),\quad i\neq j. \tag{34}$$

It can be easily shown that $t(x)$ is a monotonically increasing function of $x \geq 0$ since $dt(x)/dx = x(1+x)^{-2} \geq 0$ for $x \geq 0$. Therefore, equality in (34) holds if and only if $\gamma_i \frac{\tau_0^*}{\tau_i^*} = \gamma_j \frac{\tau_0^*}{\tau_j^*}$, $1 \leq i, j \leq K$, i.e.,

$$\frac{\gamma_1}{\tau_1^*} = \frac{\gamma_2}{\tau_2^*} = \cdots \frac{\gamma_K}{\tau_K^*} = C. \tag{35}$$

Note that $1 - \tau_0^* = \sum_{j=1}^{K} \tau_j^*$ and $\tau_j^* = \frac{\gamma_j}{\gamma_i} \tau_i^*$ from (28) and (35), respectively. Therefore, τ_i^* can be expressed as

$$\tau_i^* = (1 - \tau_0^*) \frac{\gamma_i}{\sum_{j=1}^{K} \gamma_j} = (1 - \tau_0^*) \frac{\gamma_i}{A}, \tag{36}$$

where $A = \sum_{j=1}^{K} \gamma_j$. In addition, it follows from (30), (35), and (36) that

$$\ln(1 + C\tau_0^*) - \frac{C\tau_0^*}{1 + C\tau_0^*} = \frac{A}{1 + C\tau_0^*}, \quad 1 \leq i \leq K, \tag{37}$$

where C is defined in (35). Since $C = \frac{A}{1-\tau_0^*}$ from (36), we can modify (37) as

$$z \ln z - z - A + 1 = 0, \tag{38}$$

where $z = 1 + \frac{A\tau_0^*}{1-\tau_0^*}$. It is observed that $z > 1$ if $A > 0$ and $0 < \tau_0^* < 1$. From Lemma 3.2, there exists a unique $z^* > 1$ that is the solution of (38). Therefore, the optimal time allocation to the DL WET is given by

$$\tau_0^* = \frac{z^* - 1}{A + z^* - 1}. \tag{39}$$

In addition, from (36) and (39), the optimal time allocation to the UL WITs, τ_i^*, $1 \leq i \leq K$, is given by

$$\tau_i^* = \frac{\gamma_i}{A + z - 1}. \tag{40}$$

This thus proves Proposition 3.1.

Appendix D
Proof of Corollary 3.1

It can be easily shown from (10) that $\tau_0^* = 1$ with $A = 0$. From (38) and (39), τ_0^* can be alternatively expressed as

$$\tau_0^* = \frac{z^* - 1}{z^* \ln z^*}. \tag{41}$$

Given $A \geq 0$ and thus $z^* \geq 1$, both $z^* \ln z^*$ and $z^* - 1$ in (41) increase with A since z^* increases with A as shown in the proof of Lemma 3.2 given in Appendix B. Furthermore, since $\frac{d}{dz}(z \ln z) = 1 + \ln z$ and $\frac{d}{dz}(z-1) = 1$, it follows that $\frac{d}{dz^*}(z^* \ln z^*) > \frac{d}{dz^*}(z^* - 1)$ with $z^* > 1$, i.e., $z^* \ln z^*$ increases faster with z^* than $z^* - 1$. Therefore, it can be verified that $z^* \ln z^*$ increases faster with A than $z^* - 1$, and thus τ_0^* decreases monotonically with increasing A. Finally, it can be shown that $\tau_0^* \to 0$ as $A \to \infty$ from the fact that z^* increases with A.

This thus completes the proof of Corollary 3.1.

Appendix E
Proof of Lemma 4.1

We first prove the "if" part of Lemma 4.1. If $\boldsymbol{\tau}' \in \mathcal{D}$ is a feasible solution for (12) given $\bar{R} > 0$, i.e., $R_i(\boldsymbol{\tau}') \geq \bar{R}$, $i = 1, \cdots, K$, then for any $\boldsymbol{\lambda} \geq 0$ it follows from (13) that

$$\mathcal{G}(\boldsymbol{\lambda}) \leq \mathcal{L}(\boldsymbol{\tau}', \boldsymbol{\lambda}) \leq 0,$$

and thus $\max\limits_{\boldsymbol{\lambda} \geq 0} \mathcal{G}(\boldsymbol{\lambda}) \leq 0$, which contradicts with the given assumption that there exists an $\boldsymbol{\lambda} \geq 0$ such that $\mathcal{G}(\boldsymbol{\lambda}) > 0$. The "if" part is thus proved.

Next, we prove the "only if" part of Lemma 4.1 by showing that its transposition is true, i.e, the problem in (12) is feasible if $\mathcal{G}(\boldsymbol{\lambda}) \leq 0$, $\forall \boldsymbol{\lambda} \geq 0$, by contradiction. Suppose that problem (12) is feasible and there exits an $\boldsymbol{\lambda}'' \geq 0$ where $\mathcal{G}(\boldsymbol{\lambda}'') > 0$. However, since (12) is assumed to be feasible, there exists an $\boldsymbol{\tau}'' \in \mathcal{D}$ such that $R_i(\boldsymbol{\tau}'') \geq \bar{R}$, $\forall i$, resulting in $\lambda_i''\left(R_i(\boldsymbol{\tau}'') - \bar{R}\right) \geq 0$ since $\boldsymbol{\lambda}'' \geq 0$. From (13) and (14), we thus have

$$\mathcal{G}(\boldsymbol{\lambda}'') \leq -\sum\nolimits_{i=1}^{K} \lambda_i''\left(R_i(\boldsymbol{\tau}) - \bar{R}\right) \leq 0.$$

This contradicts $\mathcal{G}(\boldsymbol{\lambda}'') > 0$, and thus problem (12) is feasible if $\mathcal{G}(\boldsymbol{\lambda}) \leq 0$, $\forall \boldsymbol{\lambda} \geq 0$. The "only if" part is thus proved.

Combining the above proofs of both "if" and "only if" parts, Lemma 4.1 thus follows.

Appendix F
Proof of Proposition 4.1

Given $\boldsymbol{\lambda} \geq 0$, the Lagrangian of problem (15) is given by

$$\mathcal{L}_{\text{WSR}}(\boldsymbol{\tau}, \mu) = \sum_{i=1}^{K} \lambda_i R_i(\boldsymbol{\tau}) - \mu\left(\sum_{i=0}^{K} \tau_i - 1\right), \tag{42}$$

where $\mu \geq 0$ denotes the Lagrange multiplier associated with the constraint in (1). The dual function of problem (15) is thus given by

$$\mathcal{G}_{\mathrm{WSR}}\left(\mu\right) = \min_{\boldsymbol{\tau}\in\mathcal{D}} \ \mathcal{L}_{\mathrm{WSR}}\left(\boldsymbol{\tau}, \mu\right). \tag{43}$$

Similar to $(\mathrm{P1})$, it can be easily shown that the problem in (15) is convex with zero duality gap. Therefore, the following KKT conditions must be satisfied by the optimal primal and dual solutions of problem (15):

$$\ln\left(1+\gamma_i\frac{\tau_0^\star}{\tau_i^\star}\right) - \frac{\gamma_i\frac{\tau_0^\star}{\tau_i^\star}}{1+\gamma_i\frac{\tau_0^\star}{\tau_i^\star}} = \frac{\mu^\star}{\lambda_i}\ln 2, \quad i=1,\ \cdots,\ K, \tag{44}$$

$$\sum_{i=1}^{K}\frac{\lambda_i\gamma_i}{1+\gamma_i\frac{\tau_0^\star}{\tau_i^\star}} = \mu^\star\ln 2, \tag{45}$$

$$\sum_{i=0}^{K}\tau_i^\star = 1, \tag{46}$$

where $\mu^\star > 0$ is the optimal dual solution. We then obtain (18) and (19) by changing variables as

$$z_i = \gamma_i\frac{\tau_0^\star}{\tau_i^\star}, \quad i=1,\ \cdots, K, \tag{47}$$

in (44) and (45), respectively. It is worth noting that $z_1 \ \cdots \ z_K$ and μ^* satisfying both (18) and (19) are uniquely determined since $K+1$ variables are solutions of $K+1$ independent equations and $\ln\left(1+z_i\right) - \frac{z_i}{1+z_i}$ is a monotonically increasing function of z_i. In addition, since $1-\tau_0^\star = \sum\limits_{i=1}^{K}\tau_i^\star$ from (46) and $\tau_i^\star = \tau_0^\star\frac{\gamma_i}{z_i}$ from (47), it follows that

$$\tau_0^\star\left(1+\sum_{i=1}^{K}\frac{\gamma_i}{z_i}\right) = 1, \tag{48}$$

from which we obtain (16). Finally, we obtain (17) from (47) and (48).

This thus completes the proof of Proposition 4.1.

REFERENCES

[1] A. M. Zungeru, L. M. Ang, S. Prabaharan, and K. P. Seng, "Radio frequency energy harvesting and management for wireless sensor networks," *Green Mobile Devices and Netw.: Energy Opt. Scav. Tech.*, CRC Press, pp. 341-368, 2012.

[2] R. J. M. Vullers, R. V. Schaijk, I. Doms, C. V. Hoof, and R. Mertens, "Micropower energy harvesting," *Elsevier Solid-State Circuits*, vol. 53, no. 7, pp. 684.693, July 2009.

[3] Y. Shi, L. Xie, Y. T. Hou, and H. D. Sherali, "On renewable sensor networks with wireless energy transfer," in *Proc. IEEE INFOCOM*, pp. 1350-1358, Oct. 2011.

[4] K. Huang and V. K. N. Lau, "Enabling wireless power transfer in cellular networks: architecture, modeling and deployment," submitted for publication. (available on-line at arXiv:1207.5640)

[5] S. H. Lee, R. Zhang, and K. B. Huang, "Opportunistic wireless energy harvesting in cognitive radio networks," *IEEE Trans. Wireless Commun.*, vol. 12, no. 9, pp. 4788-4799, Sep. 2013.

[6] L. R. Varshney, "Transporting information and energy simultaneously," in *Proc. IEEE Int. Symp. Inf. Theory (ISIT)*, pp. 1612-1616, July 2008.

[7] P. Grover and A. Sahai, "Shannon meets Tesla: wireless information and power transfer," in *Proc. IEEE Int. Symp. Inf. Theory (ISIT)*, pp. 2363-2367, June 2010.

[8] R. Zhang and C. K. Ho, "MIMO broadcasting for simultaneous wireless information and power transfer," *IEEE Trans. Wireless Commun.*, vol. 12, no. 5, pp. 1989-2001, May 2013.

[9] L. Liu, R. Zhang, and K. C. Chua, "Wireless information transfer with opportunistic energy harvesting," *IEEE Trans. Wireless Commun.*, vol. 12, no. 1, pp. 288-300, Jan. 2013.

[10] X. Zhou, R. Zhang, and C. K. Ho, "Wireless information and power transfer: architecture design and rate-energy tradeoff," to appear in *IEEE Trans. Commun.*. (available on-line at arXiv:1205.0618)

[11] A. M. Fouladgar and O. Simeone, "On the transfer of information and energy in multi-user systems," *IEEE Commun. Letters*, vol. 16, no. 11, pp. 1733-1736, Nov. 2012.

[12] S. Boyd and L. Vandenberghe, *Convex Optimization*, Cambridge University Press, 2004.

[13] R. Knopp and P. A. Humblet, "Information capacity and power control in single-cell multi-user communications," in *Proc. IEEE Int. Conf. Commun. (ICC)*, pp. 331-335, June, 1995.

[14] D. N. C. Tse and S. V. Hanly, "Multiaccess fading channels-part I: polymatroid structure, optimal resource allocation and throughput capacities," *IEEE Trans. Inf. Theory*, vol. 44, no. 7, pp. 2796-2815, Nov. 1998.

[15] L. Li and A. J. Goldsmith, "Capacity and optimal resource allocation for fading broadcast channels-part I: ergodic capacity," *IEEE Trans. Inf. Theory*, vol. 47, no. 3, pp. 1083-1102, Mar. 2001.

[16] R. Zhang, S. Cui, and Y. -C. Liang, "On ergodic capacity of fading cognitive multiple-access and broadcast channels," *IEEE Trans. Inf. Theory*, vol. 55, no. 11, pp. 5161-5178, Nov. 2009.

[17] S. Boyd, EE364b Lecture Notes. Stanford, CA: Stanford Univ., avaliable online at $\mathrm{http://www.stanford.edu/class/ee364b/lectures/ellipsoid_method_slides.pdf}$.

[18] M. Mohseni, R. Zhang, and J. M. Cioffi, "Optimized transmission for fading multiple-access and broadcast channels with multiple antennas," *IEEE J. Sel. Areas Commun.*, vol. 24, no. 8, pp. 1627-1639, Aug. 2006.

[19] A. Goldsmith, *Wireless Communications*, Cambridge University Press, 2005.